Superior cross-linking assisted layer by layer modification of forward osmosis membranes for brackish water desalination

Wafa Suwaileh[a], Daniel Johnson[a], Saeed Khodabakhshi[c], Nidal Hilal[a,b*]

[a]*Centre for Water Advanced Technologies and Environmental Research (CWATER), College of Engineering, Swansea University, Swansea, SA1 8EN, UK*

[b]*NYUAD Water Research Center, New York University Abdu Dhabi, Abu Dhabi, United Arab Emirates*

[c] *Energy Safety Research Institute, Swansea University, Bay Campus, Swansea, SA1 8EN, UK*

* Corresponding author

Abstract

In this work, a novel surface modification strategy was developed to modify polyethersulfone membrane substrate to create membranes for forward osmosis applications. A novel poly(ethylenimine) crosslinked Hexadecafluorodecanedioic acid polyelectrolyte was synthesized, followed by layer by layer deposition on the surface of an ultrafiltration membrane substrate. While the unmodified membrane was negatively charged, this procedure reversed the surface charge, leading to a positively charged forward osmosis-nanofiltration membrane. Interestingly, at pH 7, the zeta potential approached 6.9 mV for membrane coated 4.5 as compared to the pristine membrane with a zeta potential value of approximately -11.0 mV. Extensive characterization and chemical analyses were carried out to ensure the effectiveness of the developed separation layer. The results revealed that the poly(ethylenimine) crosslinked Hexadecafluorodecanedioic acid was successfully deposited on the polyethersulfone membrane substrate. Preparation conditions,

such as curing temperature and time were optimized. It was found out that membrane coated with 3.5 bilayers and cured at 60^{o}C for one hour exhibited optimal water permeability of 21.9 LMH of and solute permeability of 1.66 L m^{-2} h^{-1} as compared to the neat membrane.

Key words

Forward osmosis, brackish water desalination, polyether sulfone membrane, Layer by layer assembly, modelling.

Highlights

1- PEI modification achieved a good water flux and low RSF.

2- Superior water flux and low RSF were produced under optimal modification conditions.

3- Theoretical model predicted optimal A and B around 21.9 L m^{-2} h^{-1} bar^{-1} and 1.66 L m^{-2} h^{-1} respectively.

1 Introduction

Over the past few decades the supply of fresh water in many countries is under increasingly severe stress due to high water consumption trends [1]. To increase the production of fresh water, forward osmosis process (FO) is a viable alternative to pressure-driven membrane systems. FO can be used for water desalination, wastewater treatment, osmotic membrane bioreactors, and sludge dewatering due to low fouling tendency, simplicity of operation, and low energy requirements [2, 3]. The FO process is driven by the osmotic pressure difference between two solutions across a semi-permeable membrane [4]. This process suffers from the lack of ideal membranes with high productivity. Among the membrane candidates for FO systems, NF membranes were recently proposed to be a potential membrane having high- performance due to its high water permeation and permeate selectivity towards multivalent salts and organic molecules [5]. It is composed of a nanoscale selective layer on the top of a porous, hydrophilic, and less tortuous support layer.

A promising strategy to prepare a NF membrane with an ultrathin selective layer is the layer-by-layer (LBL) assembly process. The LBL technique involves the deposition of alternate layers of oppositely charged polyelectrolytes in repeating cycles onto a porous support [6]. Many polyelectrolyte pairs have been reported this purpose, such as poly(allylamine hydrochloride)/ polystyrenesulfonate (PAH/PSS), poly(diallyldimethylammonium chloride)/ polystyrenesulfonate (PDADMAC/PSS), poly(acrylic acid)/ poly(ethylenimine) (PAAc/ PEI), poly(ethyleneimine)/ poly(vinylsulfate) (PEI/ PVS), poly(ethyleneimine)/ polystyrenesulfonate (PEI/PSS) [7]. This method is easy to scale to design composite polyelectrolyte multilayer membranes (PEMMs) to achieve enhanced FO flux and selectivity. Even though these membranes exhibited high water permeation and acceptable retention of divalent ions such as Mg^{+2} and SO_4^{-2}, they produced poor

rejection of monovalent salts such as Na^+ [8, 9, 10, 11], due to a relatively lose selective layer. Su et al. [11] addressed this issue by modifying a porous PAN/PET substrate through LBL procedure to deposit 60 layers of poly(vinyl amine) (PVA) and poly(vinyl sulfate) that resulted in high rejection (> 90 %) of bivalent ions. However, this technique was very time consuming due to the number of repeated membrane treatments involved. In an earlier work, it was reported that a thick selective layer adversely affects the water permeability of the modified membrane [12]. As a result, the dense network structure after depositing the multilayers, cost-ineffectiveness, low stability, and low water flux restricted their use for water desalination.

An alternative approach utilizes LBL adsorption of polyacrylic acid (PAA) and polyethyleneimine (PEI) to prepare positively charged nanofiltration (NF) membranes. It is recognized that the positively charged surface can improve the rejection of divalent salt ions from feed solution and minimize scaling on the membrane surface [13]. For example, porous multilayers consisting of linear poly(ethylenimine) (LPEI) and poly(acrylic acid) (PAA) were prepared via dynamic and static LBL procedures on PES substrate. The new selective layer was smooth and performed well pervaporation application [7]. Wu et al. [5], used interfacial polymerization of PEI and trimesoyl chloride (TMC) on a polyethersulfone (PES) substrate to prepare positively charged NF membranes. Although, the selective layer was less uniform, compact, and rough, the membrane generated excellent water flux and salt rejection values of 95.1 % for $MgCl_2$, 94.4 % for $MgSO_4$, 80.5 % for Na_2SO_4 and 85.1 % for NaCl. Akbari et al. [14], developed a new strategy involving the coating of PEI on a porous PSF substrate followed by cross-linking using p-xylene dichloride (XDC) and quaternization using methyl iodide (MI). The new selective layer was uniform and was less than 3–4 μm thick. It showed good salt rejection for $CaCl_2$, NaCl, $MgSO_4$, Na_2SO_4.

In the following sections, the LBL process modification associated with cross-linking method for FO membranes will be presented. In this method, a novel PEI crosslinked HDFA was deposited on

PES substrate followed by PAA anionic layer in alternate sequence using vacuum filtration to prepare positively charged NF membranes. Thereafter, the tailored membranes were visually characterized and subjected to chemical analysis to ensuresuccessful deposition of the polyelectrolytes. The effect of the polyelectrolytes charge density on the substrate characteristics was also investigated. The membrane performance was evaluated using a cross-flow FO system. We developed a mathematical model to report the optimal values of A and B coefficients. It is worth noting that, these tailored membranes exhibited promising high water flux and acceptable reverse solute flux (RSF) after depositing 3.5 bilayers.

2 Experimental

2.1 Materials

Flat sheet polyethersulfone (PES) ultrafiltration membranes (UP150T) were utilized as a support (Microdyn-Nadir GmbH, Germany). The characteristics of the commercial UF membranes were provided by the manufacturer and they were listed in the table.1.

All the chemicals were of ACS reagent grade. Poly(acrylic acid) (Mw of 1800 g/mol) polyelectrolyte, branched Polyethylenimine (800 g/mol) and Hexadecafluorodecanedioic acid ($HOOC(CF_2)_8COOH$) (HDFA) (490.09 g/mol) cross linker agent were purchased from Sigma Aldrich (Merck). Thionyl chloride solution (118.97 g/mol), N,N-dimethyl formamide anhydrous (DMF) 99.8% (73.09 g/mol) was used as a catalyst. Triethylamine solution (anhydrous, $\geq$ 99.9 %, 101.19 g/mol, inhibitor free), tetrahydrofuran (THF) (anhydrous, ≥99.9%, 72.11 g/mol, inhibitor-free) and 2-propanol solution were used without further purification. Sodium chloride (NaCl) draw solute and sodium hydroxide (NaOH) analytical reagent were also obtained from Sigma Aldrich.

Deionized water was produced from water purification system (Millipore) and used for preparation of the polyelectrolytes and used as the feed solution.

2.2 Membrane preparation

Unmodified membranes were soaked in deionized water for one hour and then in 25% (v/v) 2-propanol solution for a further hour [15]. They were then stored in deionized water overnight. Prior to modification, the membrane was soaked in 2.0 M NaOH solution at 45 ^{o}C for one hour to hydrolyze and deposit negative charges onto the PES substrate [2].

2.3 Synthesis of PEI crosslinked HDFA

The synthesis strategy is depicted in (Fig.1). The typical synthesis process of HDFA incorporated PEI was as follows:

Thionyl chloride (50 ml) was added to 5 g of the HDFA powder under N_2. Next, dimethyl formamide (DMF, 2.5 mL) was added to the mixture and stirred under reflux at 70 ^{o}C for 24h. The solution was evaporated under vacuum until a green solid material was formed. The resulting product was dissolved in a mixture of tetrahydrofuran (THF 50 mL) and triethylamine (50 ml) under N_2. Meanwhile, the same amount of THF was mixed with PEI (10 g) and then added to the solution and stirred at 70 ^{o} C for another 24h. The crosslinked PEI was obtained by sedimenting in a centrifuge at 5000 rpm and diluted in H_2O while it was kept in a cool place for the next step.

2.4 Implementation of LBL assembly on membrane substrate

A simple vacuum assisted filtration method was performed to adsorb the LBL film onto the PES substrate [16]. Firstly, the PES substrate was placed on a Buchner funnel of the vacuum filtration with Skin layer surface side up and the backing polystyrene layer side down. The PEI crosslinked HDFA solution was deposited on to the substrate and allowed to be absorbed for approximately two hours. The substrate was subjected to thermal treatment at 60 ^{o}C for about an hour. Due to the presence of carboxyl groups in the PES substrate, as well as many amine groups in the solution, a strong electrostatic interaction was initiated forming a uniform film. The PEI was crosslinked on the PES substrate, not only to maintain permanent film, but also to increase the charged density, improve the adherence and functionality of the film.

PAA was then dispersed in DI water to prepare a concentration of 0.05 wt% anionic polyelectrolyte. It was then poured on to the first film and allowed to be adsorbed for about an hour. The alternate adsorption continued with the deposition of negatively charged PAA on the positively charged PEI/HDFA layer to create 5 bilayers. After that, the altered membranes were rinsed in DI water to remove any residues remaining on the substrate. The rinsing of membranes after completing the process is important to reverse the substrate charge. As already known, rinsing the membrane between the deposition cycles was not used because the method depends on electrostatic interaction and convective force. It should be noted that, membrane coated-PEI/HDFA film was denoted as 0.5-layer, membrane coated- PEI/HDFA + PAA film was denoted as 1.0-bilayer, and membrane coated- PEI/HDFA+ PAA + PEI/HDFA layers was denoted as 1.5-bilayers and so on.

2.5 Porosity, average pore size and structural parameter (S)

A methodology to calculate the average pore radius, and structural parameter (S) of the pristine and the altered substrates has been reported in our prior work [6].

$$S = \frac{\tau \, t_s}{\varepsilon} \tag{1}$$

In which, τ denoted the sub-layer thickness, t_s described the tortuosity, and ε represented the porosity. The porosity was quantified using this equation:

$$\varepsilon = \frac{\left(m_1 - \frac{m_2}{\rho_w}\right)}{\frac{m_1 - m_2}{\rho_w} + \frac{m_2}{\rho_p}} \text{ X } 100 \tag{2}$$

The overall porosity (ε%) of the pristine and the altered membranes was measured using a gravimetric procedure. The membranes having a size of 6 X 6 cm were soaked in DI water and then they were weighed. These membranes were subjected to freeze-drying for overnight. The weight of these frees-dried membranes was also measured. The mass difference between wet membranes (m1, g) and freeze-dried membranes (m2, g) was calculated. The density polysulfone (PS_f) material (ρ_p) is 1.00 g/cm3 while the of water (ρ_w) is 1.00 g/cm3. Equation.3 was used to calculate tortuosity.

$$T = \frac{(2 - \varepsilon)^2}{\varepsilon} \tag{3}$$

Guerout–Elford–Ferry equation was used to determine the average pore size as follows:

$$r_m = \sqrt{\frac{(2.9-1.75\varepsilon)\times 8\eta l Q}{\varepsilon \times A_m \times \Delta P}} \quad (4)$$

Where η, l, and Q described the water viscosity of 8.9 x 10^{-4} Pa s, the membrane thickness, and the volume of water permeate per unit time (m s-1) respectively. A_m (m^2) represents the effective membrane area. Note that, the hydraulic pressure (P) during the test was 1 bar.

2.6 Membrane characterization

A field-emission scanning electron microscopy (SEM) instrument coupled with energy-dispersive X-ray spectroscopy (EDS) (Hitachi high technologies corporation, Japan) and a JSM-7800 field-emission scanning electron microscope (JEOL, Japan) were used to study the morphology and microstructure of the neat and tailored membranes [17]. Before the characterization, the samples were coated by a 10 nm thin layer of platinum using a sputtering apparatus (Quorum model Q150TS) to enhance the conductivity of the tested surfaces.

An attenuated total reflectance Fourier Transform Infrared Spectroscope (ATR-FTIR, Shimadzu UK Ltd, UK) was utilized to characterize the functional groups of the PEI crosslinked HDFA material and the chemical structure of the neat and tailored surfaces [18]. The scan size of the system was ranged from 500 to 4000 cm^{-1}. Spectra of the tested material and membranes were collected using 60 averaged runs at a resolution of 4.0 cm^{-1}.

The hydrophilicity of the neat and the tailored membranes was determined using a contact angle measurement apparatus (Fibro DAT 1100, Sweden) [19]. The captive bubble method was used to obtain contact angles of both the neat and the tailored membranes. The following procedure was employed: the membrane was attached to a glass slide and it was immersed in a water bath. A J-shaped needle filled with Di water was used to generate an air bubble on the soaked selective layers in the water bath. All the contact angles values of all the examined membranes were recorded from an average of five measurements.

To quantify the surface charges of the modified and unmodified membranes, streaming potential measurements using an ElectroKinetic Analyzer (EKA, Austria) were performed [20]. Streaming potential measurements using an asymmetric cell were recorded five times at each pH. A background solution of 10 mM KCl was utilized in all the experiments. The pH of this solution was changed by adding drops of 0.1 mol/L NaOH or 0.1 mol/L HCl to investigate the difference of streaming potential with the pH of this solution. The streaming measurements were conducted at room temperature at 22 °C. After the membrane was placed in an asymmetric clamping cell, the machine was flushed using DI water and then with the electrolyte solution (10 mM KCl) for 10 minutes. Next, the pH was adjusted to a more acidic solution by adding drops of HCl solution followed by adjustment to alkaline levels by adding drops of NaOH solution.

2.7 Evaluation of membrane performance in FO system

A previously described bench-scale cross-flow FO filtration system was used to determine the water flux and reverse solute flux [6]. The water permeability coefficient and solute

permeability coefficient were computed by the classical FO model [21]. In the proposed FO process, DI water was used as a feed solution whereas different concentrations of NaCl solution (0.5, 1.0, 1.5, 2.0 mol/L) were used as a draw solution. The cleaning method of the membrane was conducted using DI water at a flow rate of 150 mL/min for 30 minutes' operation in between measurements using different concentrations of draw solution.

2.8 A new mathematical model for ranking membranes

A mathematical protocol was developed to find out the optimal A and B values for the altered membranes. Firstly, five altered membranes were prepared based on the crosslinked LBL modification method as mentioned above. These membranes were operated in the FO process to acquire the water flux and reverse solute flux results. After that, the water permeability and solute permeability coefficients were computed using MATLAB software. A second-order differential equation was used to calculate the optimal A and B values as described below [22]:

$$y'' + p(x)\, y' \, q\,(x) y = f\,(x) \tag{5}$$

When the A and B output values were plotted in the graph, equ.6 was acquired.

$$A = -0.499B^3 + 6.6423\, B^2 - 24.019\, B \tag{6}$$

Differentiation of this expression is essential to calculate the optimal A and B values as demonstrated below:

$$\frac{dA}{dB} = 0 = -3 * 0.499B^2 + 2 * 6.6423\ B - 24.019 \quad (7)$$

$$0 = \alpha x^2 + \beta x + C \quad (8)$$

$$B = \frac{-\beta \pm \sqrt{\beta^2 - 4\ a\ c}}{2a} \quad (9)$$

After solving these equations, the positive B value was only used in equ.10 to calculate the optimum A value:

$$A = -0.499\ B^3 + 6.6423\ B^2 - 24.019\ B \quad (10)$$

After identifying the optimal A and B values, the ideal membrane including the optimum number of bilayers and the optimal preparation conditions can be selected.

3 Results and discussion

3.1 Chemical analysis of PEI crosslinked HDFA

PEI is rich in amine groups which was expected to react with HDFA monomer to form strong and stable crosslinks with the substrate. To confirm the occurrence of the cross-linking among PEI and HDFA, a sample of the reacted product was analysed to identify the functional groups as shown in Fig.2. A stretching vibration peak was observed at 3362.96 cm^{-1} representing O-H bond of water [23]. The characteristic bands observed at 2938.64 and 2852.9 cm^{-1} were assigned to C–H stretching, which may represent methylene($–CH_2$) in PEI [5]. The amide-l (C=O stretching) band and amide-II(N–H) band of the amide groups (–CONH–) were clearly visible at 1647.69 and 1456.6, 1435.5 cm^{-1} wavenumbers [24]. The C-F stretching band was shifted to 1009.11 cm^{-1} as compared to the spectra reported in a prior study [23]. This indicated the successful cross-linking between PEI and HDFA mixture.

3.2 Structural characterization of modified membranes

The chemical structure of the new thin film was characterized using ATR-FTIR to identify chemical bonds. Fig.3 illustrates the spectra of the modified membranes. All the altered

membranes exhibited almost similar characteristic peaks at 2833.3, 2949.80 cm^{-1} which could be assigned to C–H stretching of methylene ($–CH_2$) in PEI. It must be pointed out that these peaks were probably overshadowing ($–CH_2$) in the PAA. Therefore, they could be ascribed to either C–H in the PEI or PAA. All new membranes exhibited similar characteristic bands. However, the intensity of these peaks was lower when applying fewer polyelectrolyte layers. The broad peaks at 3284.63 cm^{-1} are likely to indicate the presence of hydrogen bonding OH stretching region [25]. The amide-I (C=O stretching) band and amide-II(N–H) band of the amide groups (–CONH–) were clearly visible at 1649.69 and 1577.12 cm^{-1} wavenumbers as compared to Fig. (2) [5]. The small stretch vibration bond of C-F was also observed at 1041.6 and 1072.13 cm^{-1} on the substrate. This confirms the attachment of PEI and HDFA mixture forming a relatively stable thin film on the substrate.

3.3 Surface morphology and microstructure of modified membranes

Fig.4 shows that the membranes were composed of a dense selective layer on the top of a PES sublayer with finger-like structure and large macrovoids, common for UF membranes [24]. Compared to the substrate of the unmodified membrane, the newly fabricated separation layer was even, smooth, and free of defects (Fig.5). It could be suggested that the curing temperature contributed to more homogenous and uniform separation layer. When depositing more polyelectrolyte bilayers, the new separation layer became thicker, was more compacted and flatter. Similarly, increasing the coating time produced a denser and compacted structure selective layer which is in accordance with the previous work [26]. Fig.6 shows the cross-section views demonstrating the thickness of the fabricated separation layers. The thickness of the first

polyelectrolyte layer was approximately 309 nm. As the alternate deposition was continued to 5 cycles, a thicker separation layer of 1.5 μm was formed.

Modified membranes showed similar microstructures of large voids and finger like structure as compared to the unmodified membrane. However, there are small aggregates forming shapeless clusters were visible between the macrovoids due to the penetration of polyelectrolytes into the pores (Fig.7.). This can cause some pore blocking which in turn decreases the apparent porosity of the sublayer.

3.4 Hydrophilicity of modified membranes

It can be seen from table.1, the variation in water contact angle as successive bilayers are formed on the surface. The results revealed that grafting a bilayer of PEI/HDFA on the substrates caused a dramatic decrease in water contact angle to 50.8 ^{O} ± 1.1 compared to 60.4^{o} ± 1.6 for the unmodified membrane. The water contact angle continued to decrease to 35.8 ^{O} ± 0.82 after grafting 5 positively charged bilayers, indicating improved hydrophilicity. Also, Yang et al. [26] stated that the contact angle was decreased remarkably due to the deposition of PEI layer on the membrane surface. A possible reason for this low contact angle could be caused by the increased number of amine groups in the 4.5 LBL substrate. Therefore, the substrate had high affinity to water molecules leading to more a hydrophilic separation layer. This good hydrophilicity may promote the transfer of water flux within the sublayer and to the interface of the separation layer.

3.5 Zeta potential for evaluating coating efficacy

The zeta potential for the modified membranes was studied to explore the effect of the pH of the alkaline solution to the membrane surface charge and how surface charges contribute to the salt rejection. It is obvious from Fig.8 that the zeta potential of the first coating layer was remarkably shifted to 1.4 at a pH value of 4.4. It was observed that the zeta potential of this membrane was increased rapidly in the acidic region. Interestingly, the increased number of multilayers of PEI resulted in the positively charged membrane at neutral pH value. As indicated in the same figure, the curves appeared very similar and the zeta potential was still significantly higher for 2.5, 3.5, and 4.5-bilayer membranes at pH values less than 7.0. For example, the zeta potential reached a maximum value of 38.6 mV for 4.5 LBL membrane, leading to a desirable highly positively charged surface. It should be noted that the density of the positive charges on the modified substrates approached its maximum after applying 4.5 bilayers. The excess of positive charge on the membrane surface can be ascribed to a high amount of abundant positively charged amino groups in the PEI coating layer [27]. Additionally, the drastic maximization of the positive charges can be elucidated by the high protonation of amine groups when the pH value of the solution became more acidic.

The above results indicated that an electrostatic repulsion would have occurred between divalent salts and membrane surface as these salts had identical charge similar to the membrane. Thus, these salt cations can be rejected easily from the membrane surface. It is therefore expected that this electrostatic repulsion between scale precursors such as Ca^{+2}, Mg^{+2} in the brackish water as the FS and the positively charged substrate would potentially impart the modified membrane with lower salt scaling/fouling.

It should be noted that Na^{+1} had a similar charge as the membrane but exhibit a weak repulsion force that results in a low salt rejection ratio. This can be assigned to the electro-neutrality condition as these cations were transported from the greater charge concentration region to the lower charge concentration region until electro-neutrality on both sides of the membrane was achieved [28]. The

basic conclusion that can be extracted from the above discussion was that if these positively charged membranes will be used in a basic solution such as brackish water, they may achieve good salt rejection ratio toward divalent ions and minimum scaling/fouling on the membrane surface. It must be mentioned that; the zeta potential can be influenced by the type of salt ions, the concentration of salt ions in the feed solution, and adsorption of the dissolved ions on the membrane surface.

3.6 Effect of multilayer polyelectrolytes on substrate pore size and porosity

To evaluate the effect of the polyelectrolyte modification on the porosity of the sublayer, the mean pore size was determined for all altered membranes. It was found that the first bilayer coating showed insignificant decrease in the mean pore size (see Fig.9). This is because the adoption of the first polyelectrolyte pair would not entirely block the pores, but a superficial obstruction might occur. Such a result was reported previously [29]. He postulated that the polyelectrolyte solution would clog some of the entire pores of the sublayer. Furthermore, the thin film had a loose structure, was less uniform, and demonstrated high permeability.

In contrast, depositing multilayer polyelectrolytes resulted in a drastic reduction in the porosity of the sublayer governed by high diffusivity of the polyelectrolytes into the pathways of the sublayer (see Fig.7). The addition of more polyelectrolyte layers yielded an observed range of pore size from 72.1 (0.5 layer) to 32.7 nm (4.5 LBL) (calculated by equ.4). Pore clogging probably occurred between interconnected pores because the polyelectrolyte solution could have easily penetrated and intersected with pores junction after depositing 4.5 bilayers. This may have caused a decrease in the porosity and number of macrovoids in the sublayer. It was found out that the porosity was decreased from 60 % to 49 % (calculated by equ.2) after depositing 4.5 LBL

on the membrane surface. This means that the polyelectrolyte solution was adsorbed to the pore surfaces and blocked them due to its low viscosity and the formation of tiny aggregates. According to Arena et al. [30], the coating solution can penetrate through the entire pores and form agglomeration. This resulted in pore blocking between interconnected pores of the sublayer. Although the porosity was decreased when applying more polyelectrolyte multilayers, the reverse solute flux far exceeds that for the neat membrane. Furthermore, high water flux was obtained due to greater hydrophilicity and lower surface energy resistance as compared to the pristine membrane [30]. However, the water flux was declined slightly when applying polyelectrolyte multilayers to the substrate. It can be suggested that the membrane performance was correlated with mean pore radius rather than hydrophilicity.

3.7 Effect of coating time and temperature on membrane performance

The heat post-treatment temperature and coating time played a crucial role in defining the membrane productivity. These conditions were adjusted to improve the interaction efficiency between amine groups in PEI and carboxyl groups with the PAA on the substrate. Also, the heat treatment induced an additional cross-linking between PEI and HDFA on the substrate and maintained a stable film. It was found that the heat treatment contributed to the stability of the coating layer with little enhancement to the membrane performance which is complying with in the previous results [5]. In this research, the temperature ranged from 40 ^{o}C to 70 ^{o}C. The water flux and reverse solute flux results for DI water FS and 1 mol/L NaCl DS are plotted in Fig. 10. It can be seen that the best water flux was achieved for membrane cured at 60 ^{o}C followed by a reduction at higher curing temperatures. To further optimize the curing time, the modified membranes were exposed to a temperature of 60 ^{o}C for 30 minutes, 1 hour, 1.5 hour, and 2 hours.

Figs. 10(A-B) shows membranes cured at 60 ^{o}C for an hour demonstrated the best water flux and stable reverse solute flux. This is because the heat treatment improved the uniformity and probably decreased the pore size appreciably, resulting in better selectivity of the developed film. Consequently, thermal treatment at 60 ^{o}C and curing time of an hour were the optimal conditions for this surface modification method.

4 Osmotic performance of the modified membranes

The separation performance of the membranes modified with polyelectrolyte multilayers in the is summarized in Figs. (11A-B). The water permeation dropped slightly after depositing the first positively charged PEI layer. However, a decrease in the reverse solute flux by approximately 20% was observed. The results revealed that the water flux was 20.1, 22.2, 24.8, and 17.6 L m^{-2} h^{-1} when using DI water as FS and 0.5, 1.0, 1.5, and 2.0 mol/L NaCl as a DS as compared to that from the neat membrane. The membrane produced a reverse solute flux of 30.5, 53.7, 85.2, 36.2 g/m^2.h when utilizing DI water as FS and 0.5, 1.0, 1.5, and 2.0 mol/L NaCl as DS as compared to that from the unmodified membrane. A further reduction in the water permeation and reverse solute flux was observed after applying multilayer polyelectrolytes on the substrate. As expected, the order of water flux and reverse solute flux of all the altered membranes were as follows: B-0.5 > B-1.5 > B-2.5 > B-3.5 > B-4.5. According to the literature, the reduction in the water flux was attributed to the high mass resistance of the thick polyelectrolyte multilayer on the membrane surface [26].

Moreover, the decrease in water flux can be ascribed to blocking of pores by build-up of PEI material within the membrane structure, causing an increase in the water transport resistance while hampering the transport of some salt ions. When some pores were blocked during the coating process, the tortuosity of the sublayer was increased yielding high ICP effects. As

mentioned by another study [31], not all PEI molecules would be adhered to the substrate because of the electrostatic repulsion among similar charged polyelectrolytes. We suggest that in this work, the first bilayer was not continuous on the substrate and could have been bonded weakly to the substrate, resulting in lower charge density. As might be expected that, the tighter mean pore size could have contributed to a slight reduction in the water flux and the reverse solute flux.

Conversely, there was a further increase in the water permeation and reverse solute flux when the concentration of the DS was increased to 1.5 mol/L, whilst a large drop in these values was observed at 2.0 mol/L DS. This could be a result of the superfast water/solute transfer through the pores which caused trapping of salt ions leading to ICP induced reduction of water transport [-6]. After the second deposition of PEI polyelectrolyte, the water flux began to drop slowly while a large variation was noted at high DS concentration of 2 mol/L NaCl. With a further increase in the sequential depositions of PEI/PAA bilayers, the water flux decreased by 35%, along with a reduction in the reverse solute flux, as shown by the water/salt fluxes in Figs.11A-B. When the substrate was coated with 4.5 PEI bilayers, the water flux varied significantly. It was seen that the water flux was sharply reduced to 12.8, 14.5, 16.1, and 11.7 L m^{-2} h^{-1} whereas the reverse solute flux achieved 18.0, 22.5, 28.7, and 25.3 g/m^2.h, when using DI water as FS and 0.5, 1.0, 1.5, and 2.0 mol/L NaCl as a DS respectively. A possible reason for this decrease in the water flux could be that the PEI molecules were overlapped and rearranged on the substrate leading to a thicker and more compacted film. According to earlier research [32], a denser film could be influenced by the ionic strength of the polyelectrolyte solution it is subjected to.

The increase in the water permeation was accompanied by an increase in the solute reverse flux showing typical trade off phenomena. The severe effect of ICP and salt accumulation within the

sublayer significantly influenced the water transport, particularly at high DS concentration. Although the concentration of the DS was increased, a similar trend of low water/solute permeability was found, due to incorporating multilayer polyelectrolytes. There was a correlation between the number of polyelectrolyte layers and the water/solute permeability values for all modified membranes. The best membrane performance can be assigned to membranes with 3.5 cycles of bilayer deposition.

5 Determination of the optimal membrane transport parameters

The intrinsic separation properties of the modified membranes are illustrated in Fig.12. They were computed according to the model established by a group of researchers [21]. Since there was no specific method to identify the acceptable intrinsic permeability parameters, a range of A values were plotted against B values using a quadratic fit that identified the optimal values.

The same observations can be made for water permeability and solute permeability. For all the modified membranes, these parameters were higher upon increasing the concentration of the draw solution. Despite that, the values were markedly reduced when using concentrated draw solution of 2.0 mol/L NaCl. In comparison to the surface modification protocol reported in our previous work, the PEI cross-linked HDFA membranes showed lower optimum A value and higher optimum B values of 21.9 L m^{-2} h^{-1} bar $^{-1}$ and 1.66 L m^{-2} h^{-1} respectively. The optimum number of deposition cycle was 3.5 polyelectrolyte bilayers. However, although many deposition cycles were required to manufacture the selective layer, there was room to further maximize the water permeability and minimize the solute permeability through advancing the modification conditions and strategy.

6 Conclusions

PES membranes were modified via LBL adsorption using positively charged PEI polyelectrolyte cross-linked with HDFA and negatively charged PAA polyelectrolyte to form an effective selective layer for use as FO membranes. Through using this modification protocol, it was possible to fabricate a positively charged FO membrane that contributed to lower reverse solute flux.

The characterization results revealed that the PEI cross-linked HDFA was successfully deposited on the PES substrate, forming a homogenous and uniform selective layer. This procedure improved the hydrophilicity of the membrane significantly, resulting in a relatively high water flux which declined by approximately 10% as each successive polyelectrolyte bilayer was deposited. A decline in the average pore size of the sublayer coated with polyelectrolyte multilayers from 83.2 to 32.7 nm was also observed. This contributed to lower reverse solute flux at the expense of reduced water flux due to tight pores along with pore clogging phenomena.

It was found that the optimal heat treatment and curing time were 60 ^{o}C and an hour. The newly developed membranes exhibited a high optimal A value of 21.9 L m^{-2} h^{-1} bar^{-1} and a comparable B value of 1.66 L m^{-2} h^{-1}. This also indicated that the optimal number of polyelectrolyte bilayers was 3.5 bilayers. Although this modification approach is believed to be promising for fabricating an efficient FO membrane, more research is still needed to optimize the cross-linker concentration, pH value, the stoichiometric ratio between PEI and HDFA and cross-linking time. Further experiments are needed to investigate the influence of ions concentrations in brackish water feed on the zeta potential to get a clearer vision on the salt rejection mechanisms.

Acknowledgments

The authors would like to thank Qatar Foundation for Education, Science and Community Development for providing PhD scholarship to W. Suwaileh

Figure Captions

Figure.1: Schematic drawing of the synthesis process and layer-by-layer assembly on a PES membrane.

Figure.2: ATR-FTIR spectra for unmodified membrane substrate and PEI crosslinked HDFA product. Indicative peaks of PEI at 1456.6 and 1647.69 cm^{-1}. Indicative peaks of HDFA at 1456.6 and 1009.11 cm^{-1}.

Figure.3: ATR-FTIR spectra for pristine membrane substrate, bilayer and trilayer membranes with different numbers of polyelectrolyte layers.

Figure.4: Cross sectional images of a modified membrane showing a finger like shape and large macrovoids.

Figure.5: Morphology of the unmodified membrane and the membranes treated with multilayer positively charged polyelectrolytes.

Figure.6: Cross sectional images of substrates coated with 0.5 and 4.5 polyelectrolyte bilayers. The thickness of the selective layer ranged from 309 nm to 1.5 μm.

Figure.7: (a) Showing polyelectrolyte solution penetrated into the sublayer causing pore clogging. (b) Cross-sectional pore morphology of the tailored membrane.

Figure.8: Zeta potential measurements of all the positively charged LBL assembled membranes.

Figure.9: A trend of average pore size for all treated membranes with multilayer polyelectrolytes.

Figure.10: (a) Variation of water flux and solute reverse flux with different curing temperatures for LBL coated membrane. (b) Variation of water flux and solute reverse flux with different curing time for LBL coated membrane.

Figure.11: Separation performance of the pristine membrane and all positively charged membranes at varying NaCl concentrations as a DS and DI water as a FS (a) water flux (b) solute reverse flux.

Figure.12: Modeling outputs of A and B values using the typical FO theoretical model, with a quadratic fit for determination of the optimal A and B values.

Graphical abstract

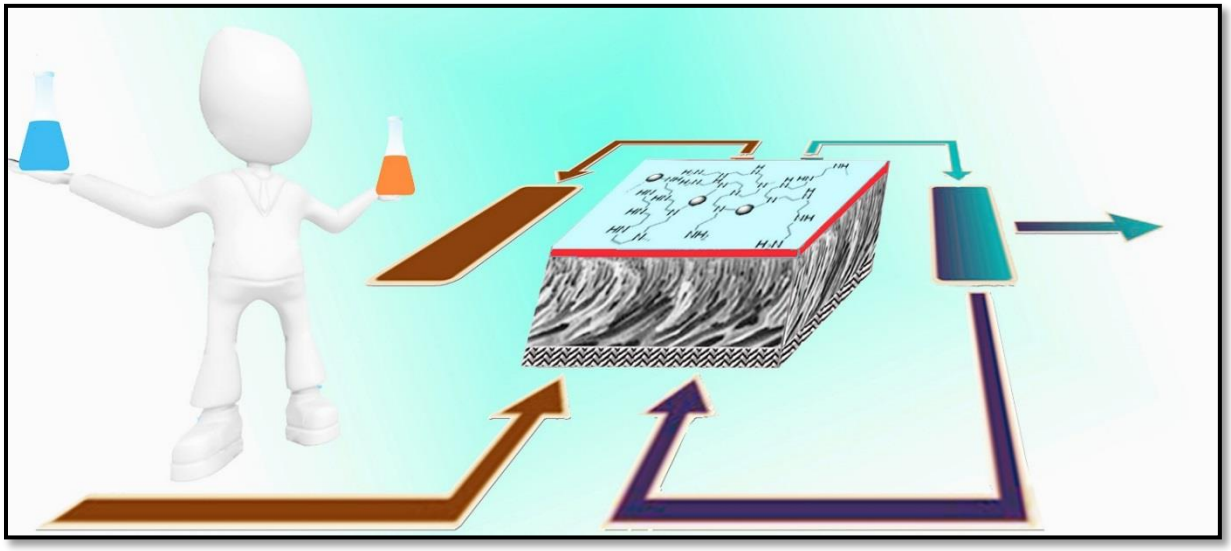

Figure.1

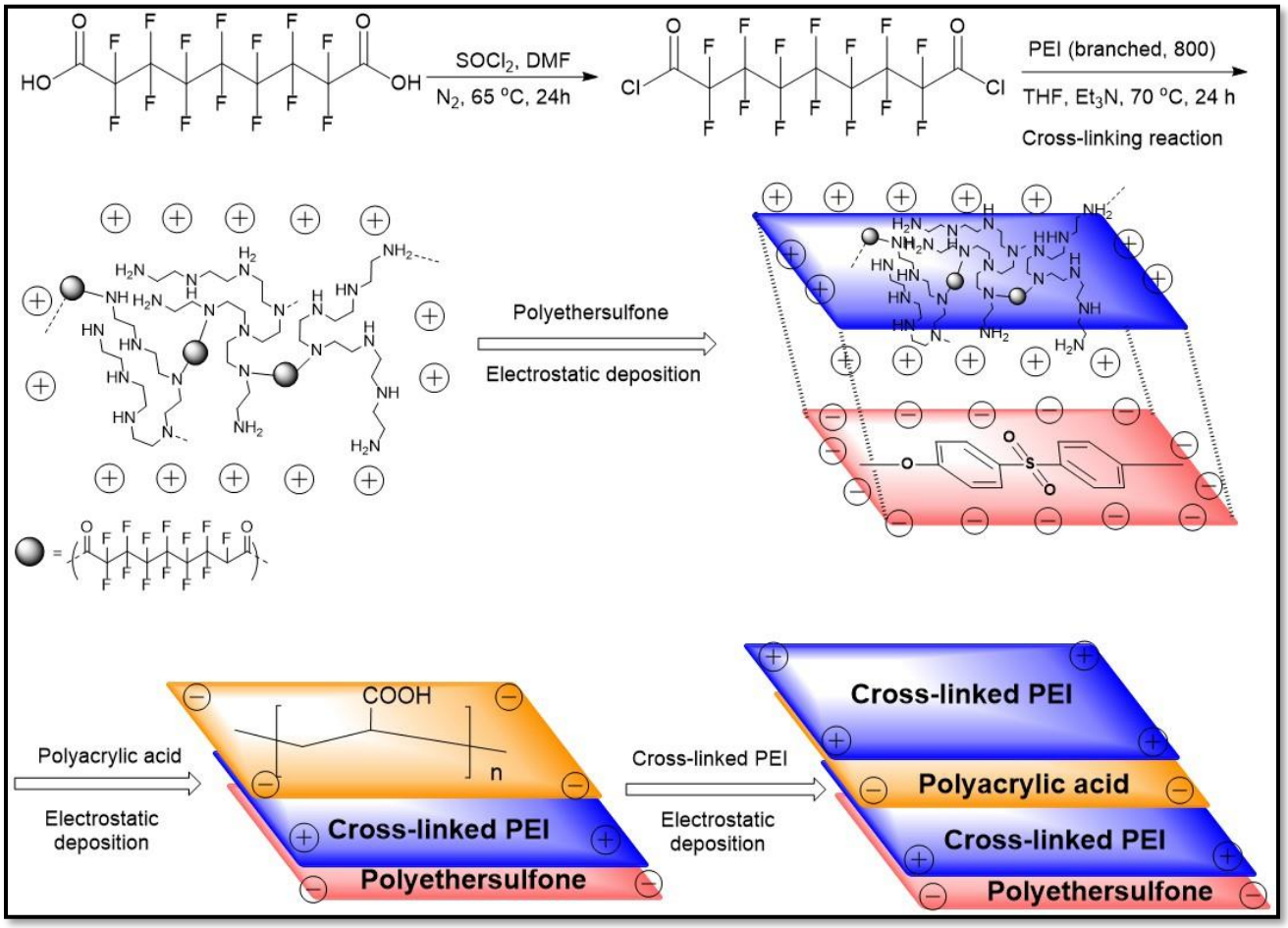
SOCl2, DMF
N2, 65 °C, 24h
PEI (branched, 800)
THF, Et3N, 70 °C, 24 h
Cross-linking reaction
Polyethersulfone
Electrostatic deposition
Polyacrylic acid
Electrostatic deposition
COOH
Cross-linked PEI
Polyethersulfone
Cross-linked PEI
Electrostatic deposition
Cross-linked PEI
Polyacrylic acid
Cross-linked PEI
Polyethersulfone

Figure.2

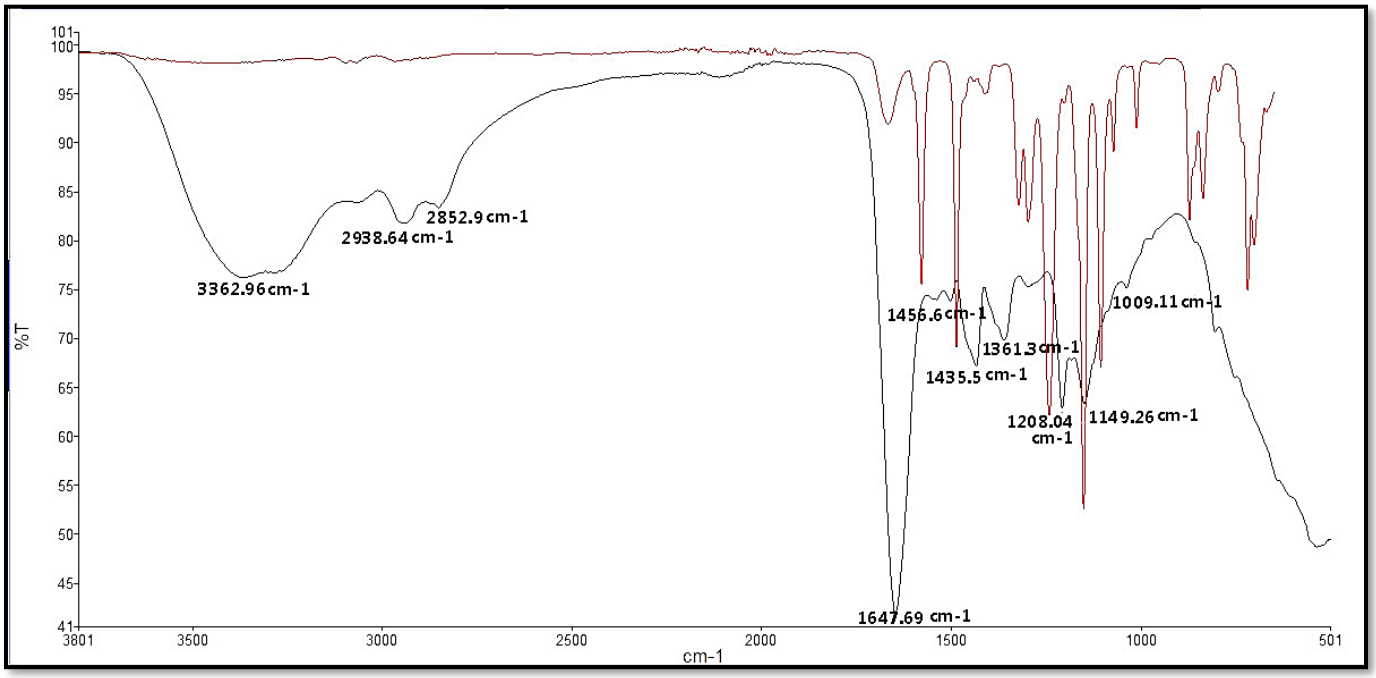
%T
cm-1
3362.96 cm-1
2938.64 cm-1
2852.9 cm-1
1647.69 cm-1
1456.6 cm-1
1435.5 cm-1
1361.3 cm-1
1208.04 cm-1
1149.26 cm-1
1009.11 cm-1

Figure.3

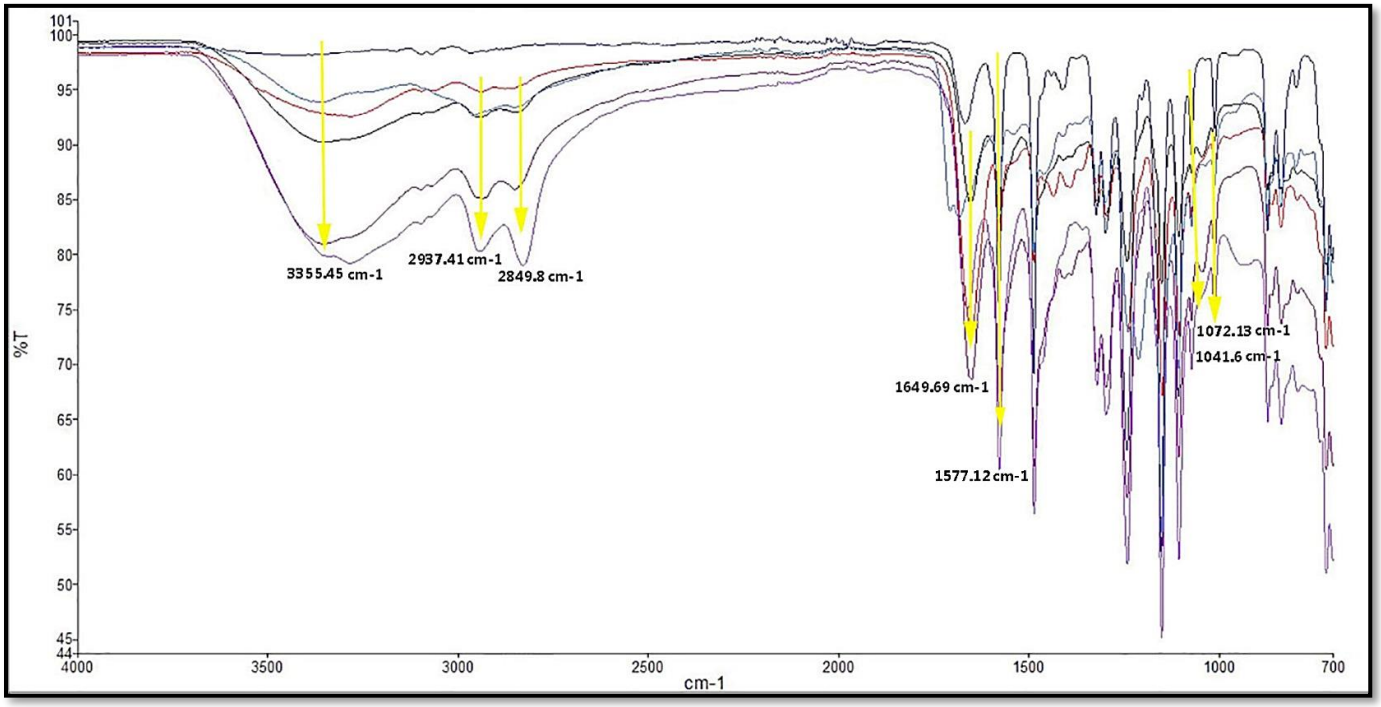
%T
cm-1
3355.45 cm-1
2937.41 cm-1
2849.8 cm-1
1649.69 cm-1
1577.12 cm-1
1072.13 cm-1
1041.6 cm-1

Figure.4

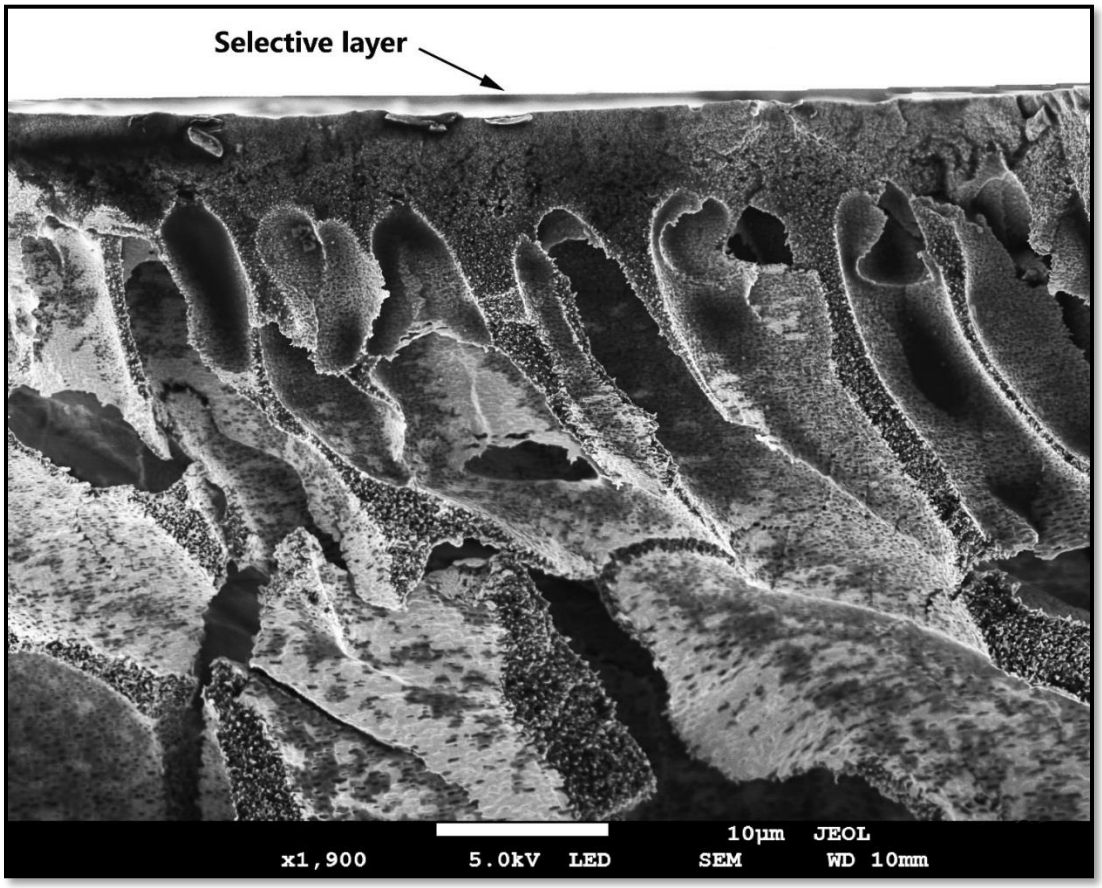

Figure.5

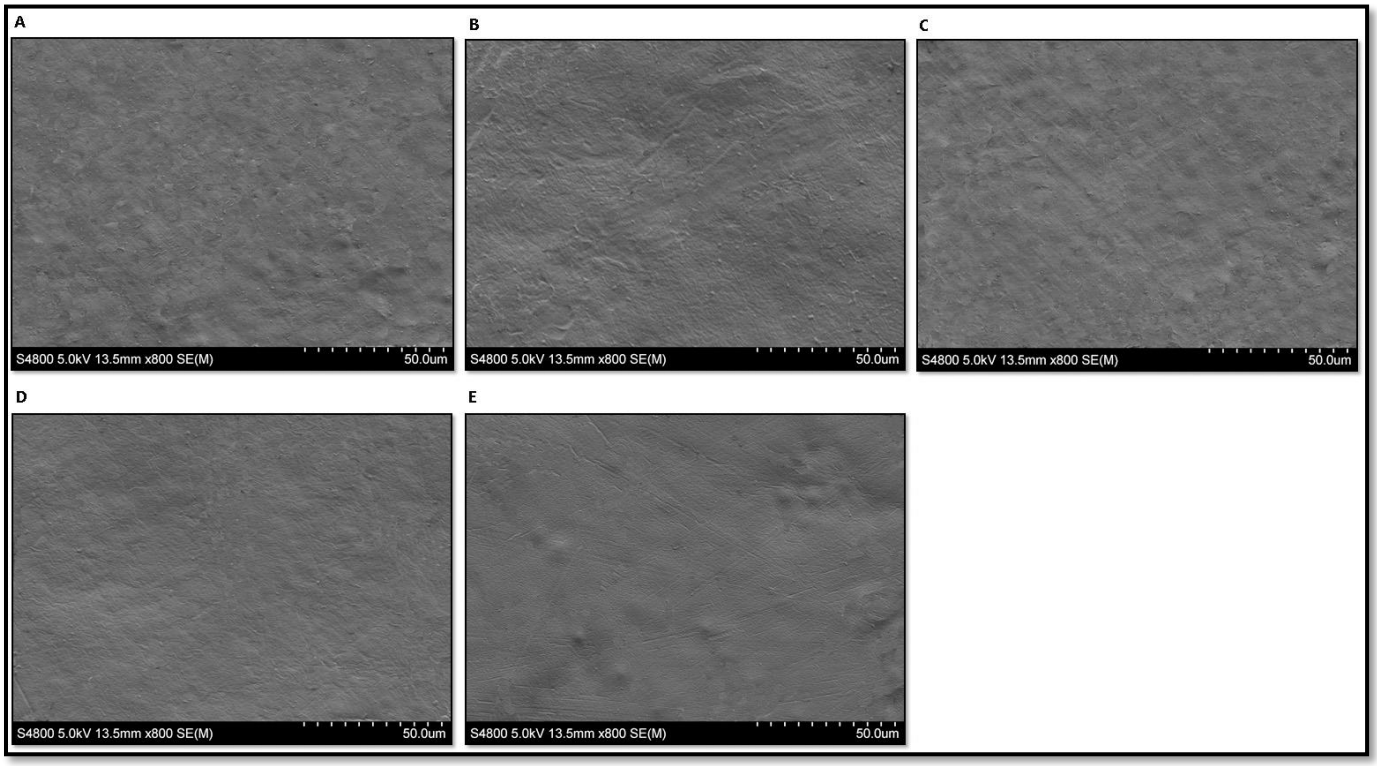
A
S4800 5.0kV 13.5mm x800 SE(M)
50.0um
B
S4800 5.0kV 13.5mm x800 SE(M)
50.0um
C
S4800 5.0kV 13.5mm x800 SE(M)
50.0um
D
S4800 5.0kV 13.5mm x800 SE(M)
50.0um
E
S4800 5.0kV 13.5mm x800 SE(M)
50.0um

Figure.6

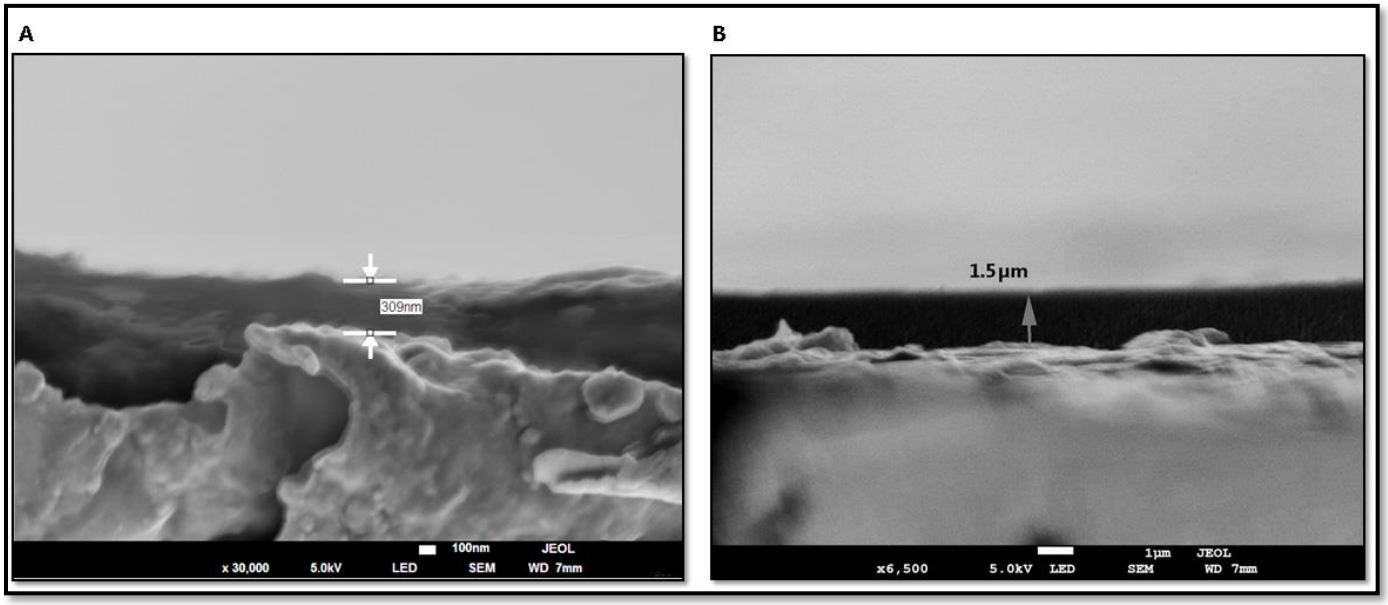
A
309nm
100nm
JEOL
x 30,000
5.0kV
LED
SEM
WD 7mm
B
1.5µm
1µm
JEOL
x6,500
5.0kV
LED
SEM
WD 7mm

Figure.7

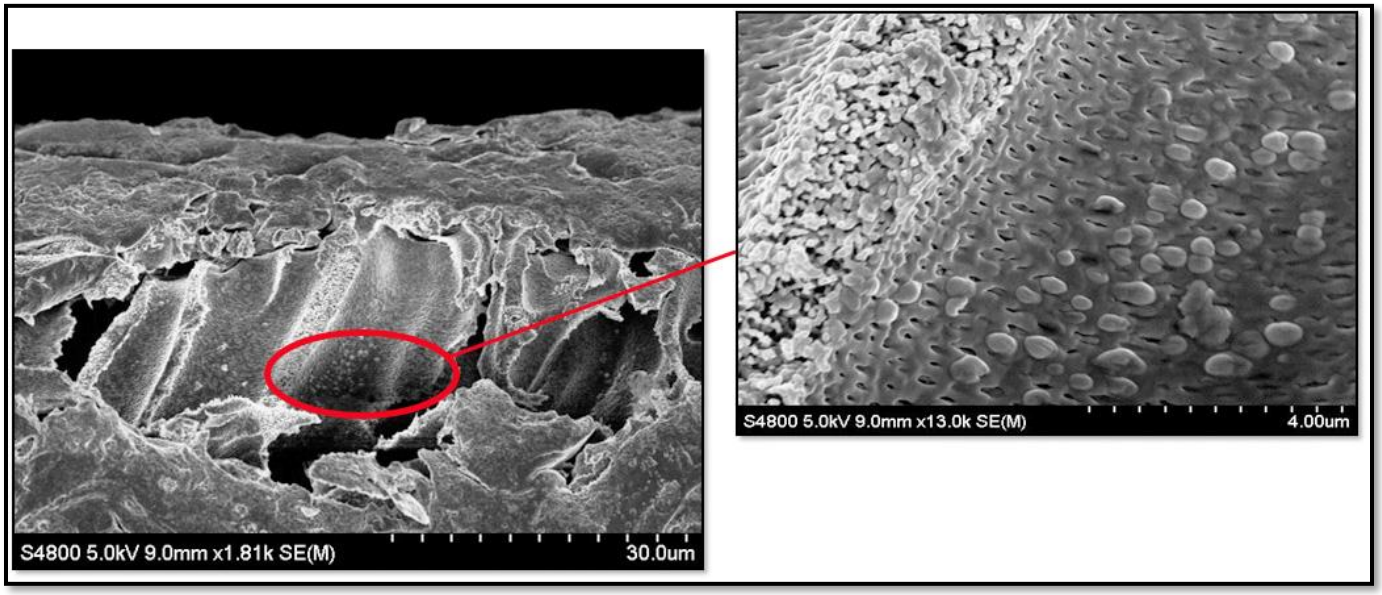
S4800 5.0kV 9.0mm x1.81k SE(M)
30.0um
S4800 5.0kV 9.0mm x13.0k SE(M)
4.00um

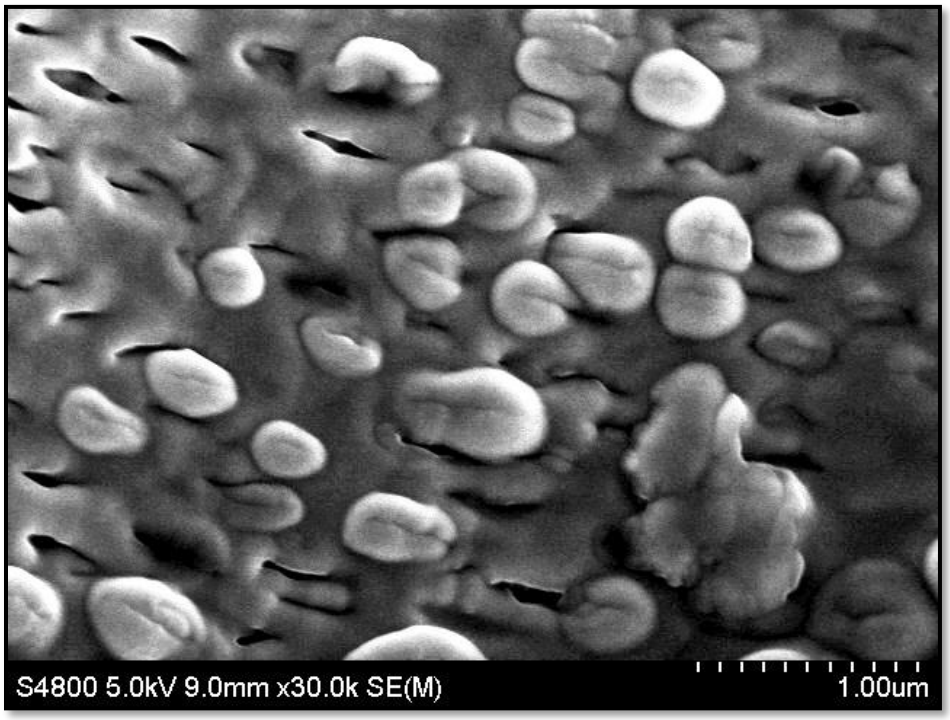
S4800 5.0kV 9.0mm x30.0k SE(M)
1.00um

Figure.8

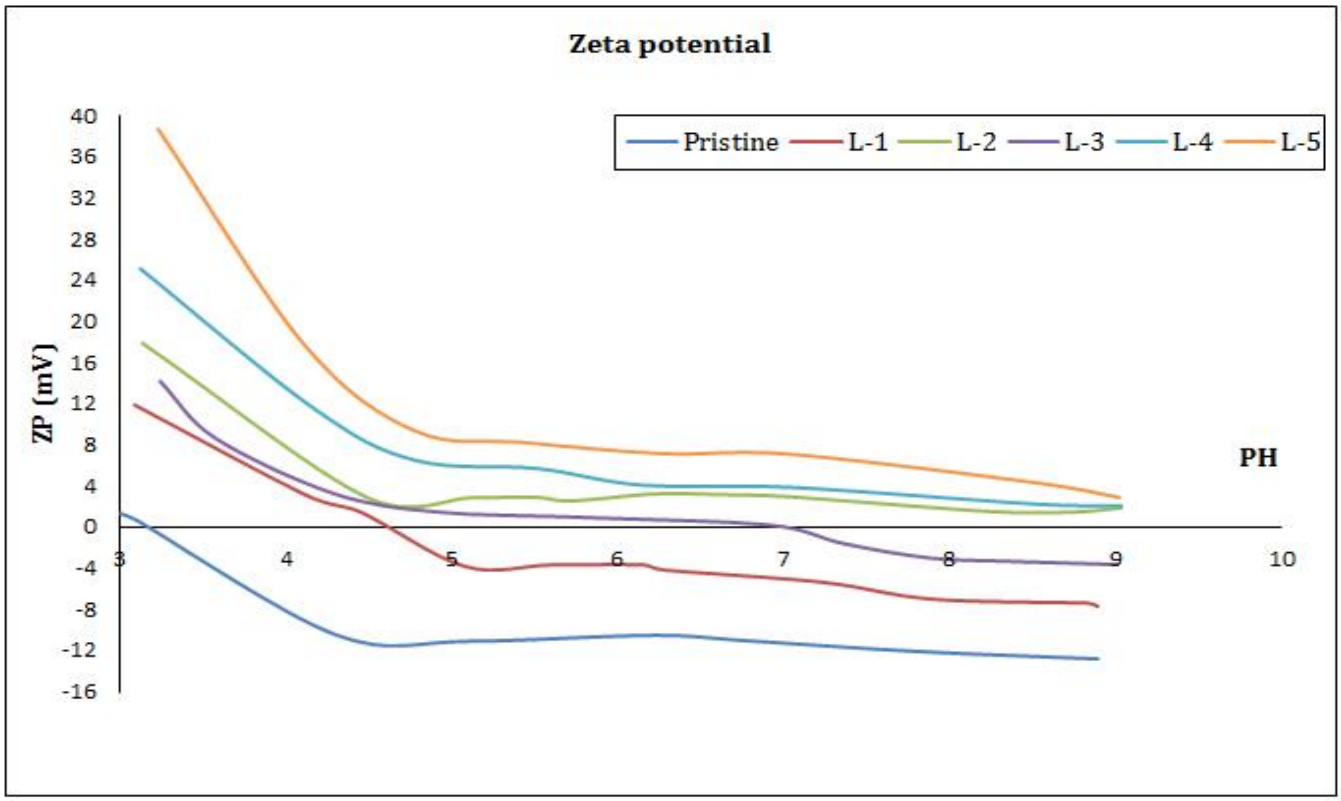
Zeta potential
Pristine
L-1
L-2
L-3
L-4
L-5
ZP (mV)
PH
40
36
32
28
24
20
16
12
8
4
0
-4
-8
-12
-16
3
4
5
6
7
8
9
10

Figure.9

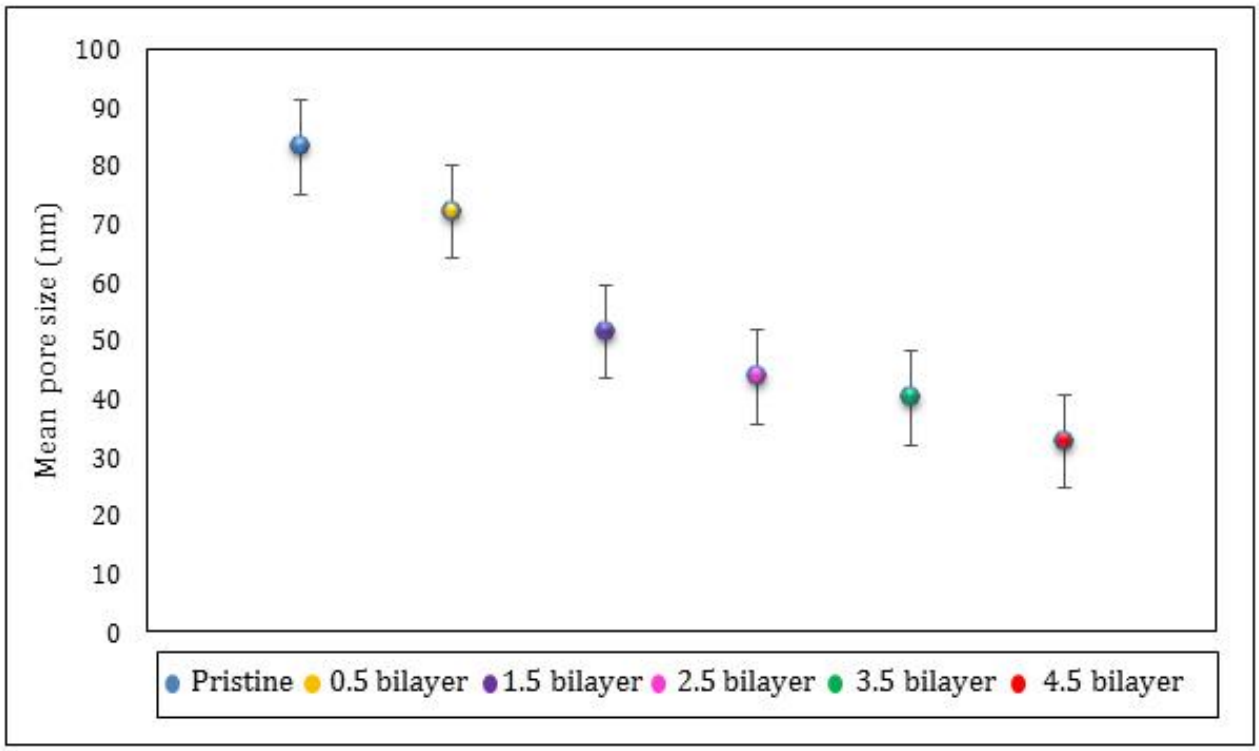
Mean pore size (nm)
100
90
80
70
60
50
40
30
20
10
0
Pristine
0.5 bilayer
1.5 bilayer
2.5 bilayer
3.5 bilayer
4.5 bilayer

Figure.10

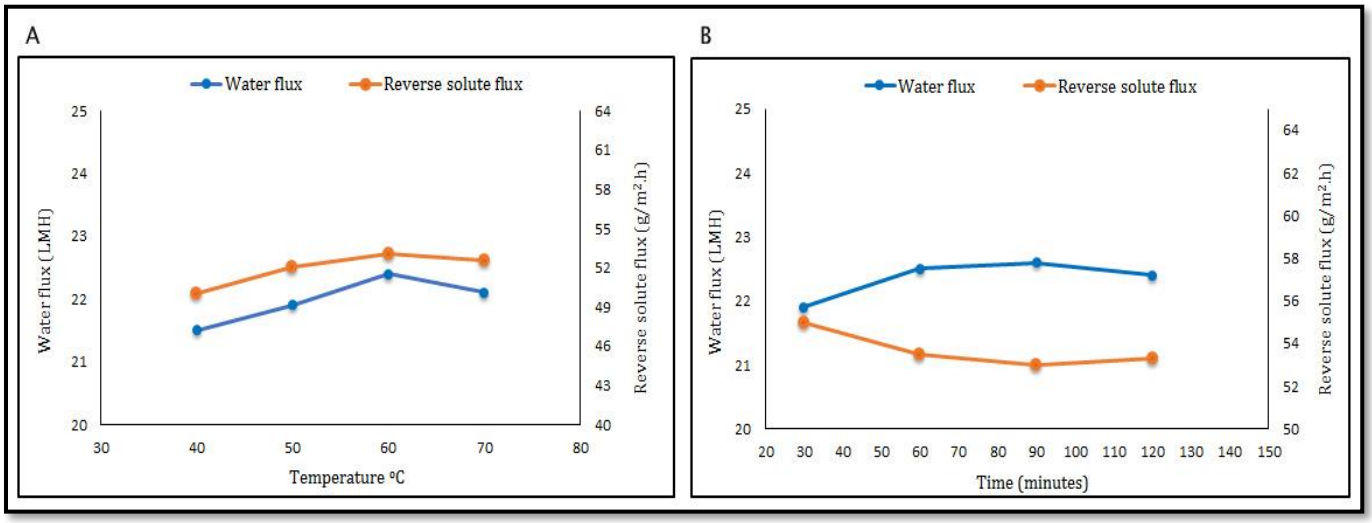
A
Water flux
Reverse solute flux
Water flux (LMH)
Reverse solute flux (g/m².h)
Temperature °C
B
Water flux
Reverse solute flux
Water flux (LMH)
Reverse solute flux (g/m².h)
Time (minutes)

Figure.11

A

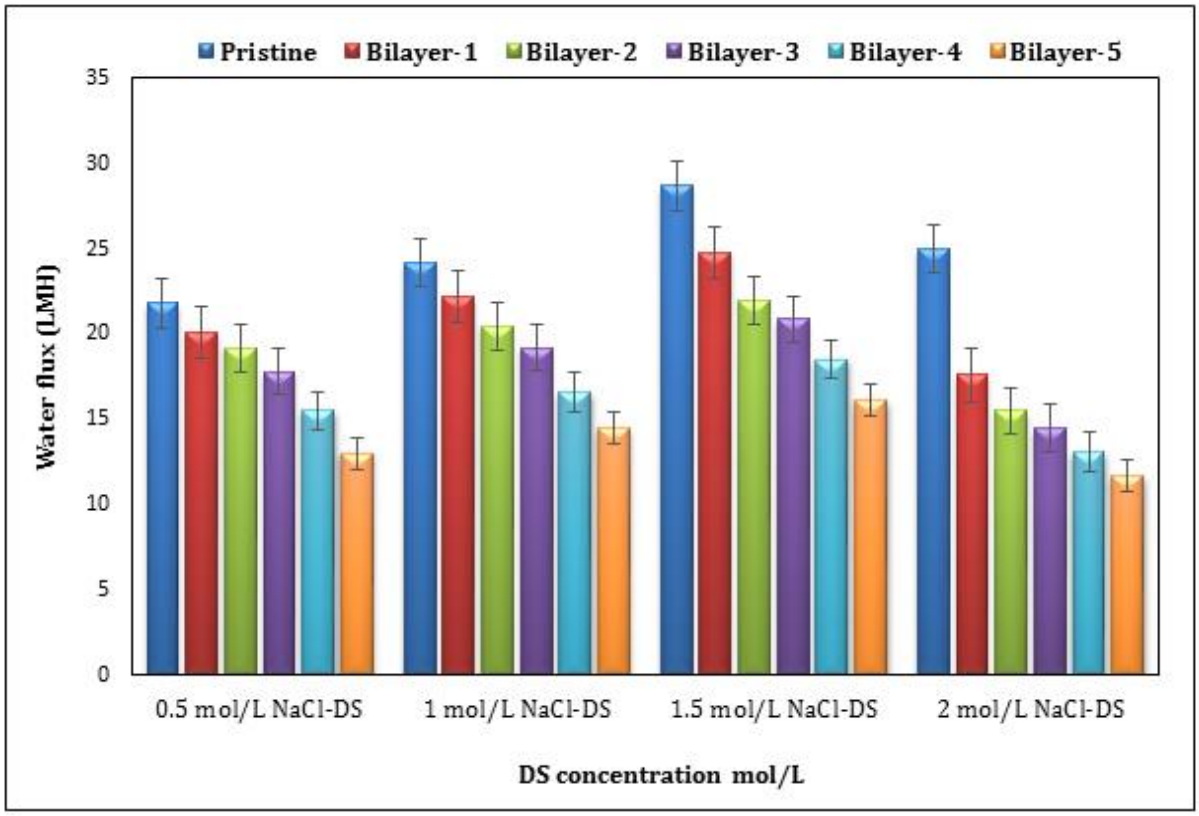
Pristine
Bilayer-1
Bilayer-2
Bilayer-3
Bilayer-4
Bilayer-5
Water flux (LMH)
35
30
25
20
15
10
5
0
0.5 mol/L NaCl-DS
1 mol/L NaCl-DS
1.5 mol/L NaCl-DS
2 mol/L NaCl-DS
DS concentration mol/L

B

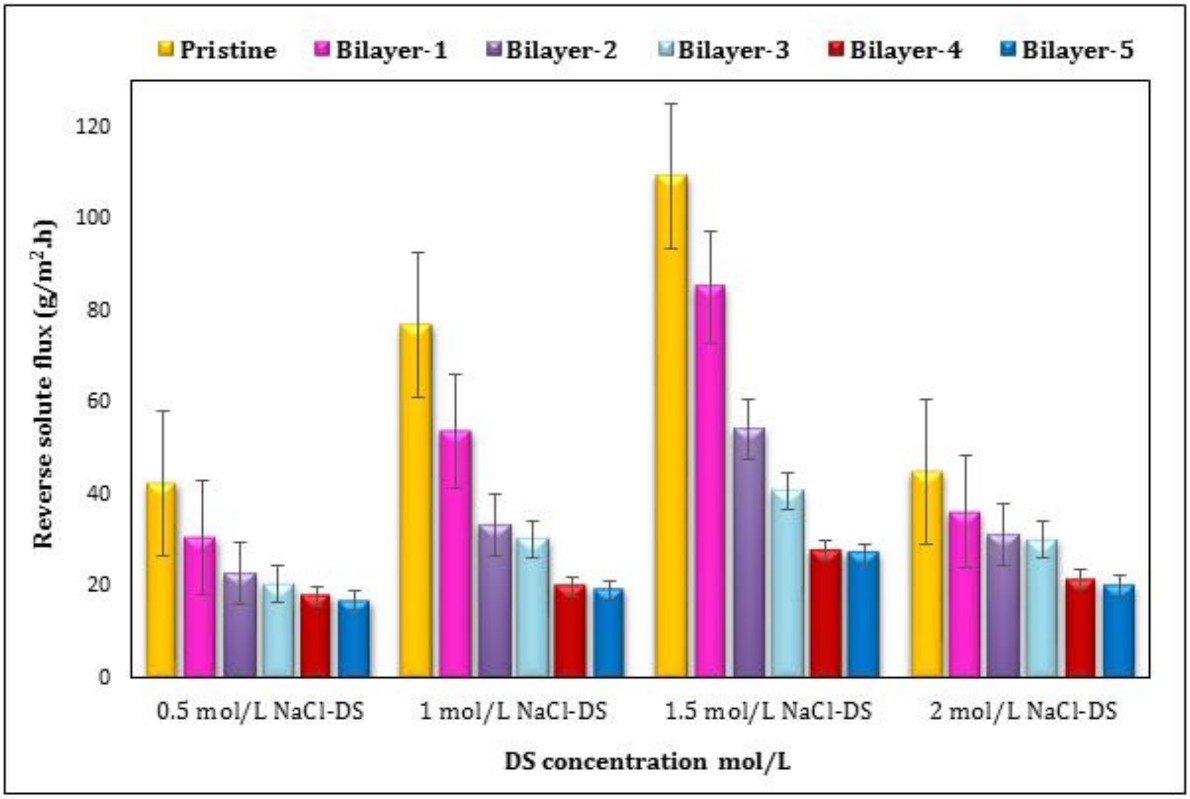
Pristine
Bilayer-1
Bilayer-2
Bilayer-3
Bilayer-4
Bilayer-5
Reverse solute flux (g/m2.h)
120
100
80
60
40
20
0
0.5 mol/L NaCl-DS
1 mol/L NaCl-DS
1.5 mol/L NaCl-DS
2 mol/L NaCl-DS
DS concentration mol/L

Figure.12

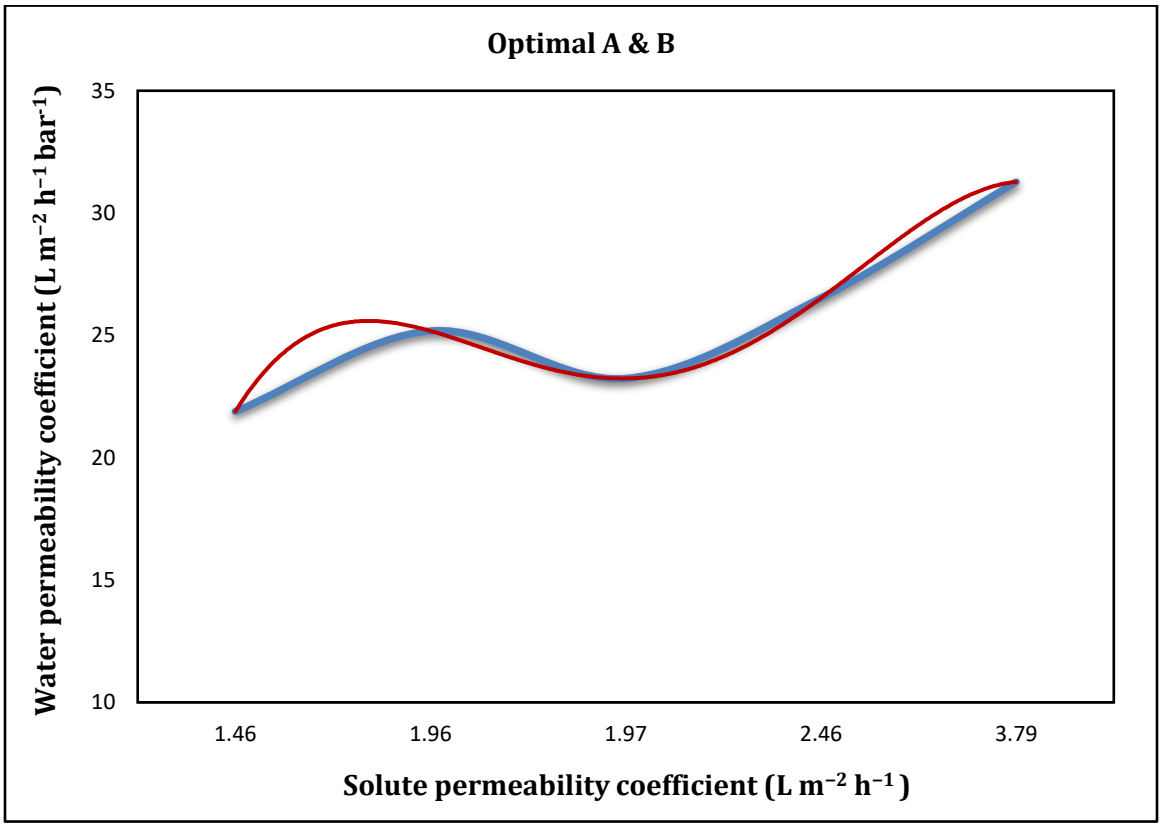
Optimal A & B
Water permeability coefficient (L m⁻² h⁻¹ bar⁻¹)
35
30
25
20
15
10
1.46
1.96
1.97
2.46
3.79
Solute permeability coefficient (L m⁻² h⁻¹)

List of tables:

Table.1: The characteristics of the commercial UF membrane.

Material	**Polyether sulfone (PES)**
Backing support	polyester
Molecular weight cut off (Da)	150,000
Thickness (μm)	210-250
Water permeability (LMH/bar)	$\geq$ 285
Retention PVP K85 (%)	90.0 – 98.0

Table.2: Contact angles for the pristine and the new positively charged membranes.

Number of bilayers	**Contact angles**
Pristine	58.9
0.5	50.8
1.5	49.9
2.5	46.9
3.5	41.3
4.5	35.8

References

[1] P.S. Goh, A.F. Ismail, N. Hilal, Nano-enabled membranes technology: Sustainable and revolutionary solutions for membrane desalination?, Desalination 380 (2016) 100–104.

[2] S. Kwon, J. S. Lee, S. J. Kwon, S. Yun, S. Lee, J. Lee, Molecular layer-by-layer assembled forward osmosis membranes, Journal of Membrane Science 488 (2015) 111–120.

[3] Y. Choi, J. Choi, H. Oh, S. Lee, D. R. Yang, J. Ha Kim, Toward a combined system of forward osmosis and reverse osmosis for seawater desalination, Desalination 247 (2009) 239–246.

[4] Sh. Zhao, L. Zou, D. Mulcahy, Brackish water desalination by a hybrid forward osmosis–nanofiltration system using divalent draw solute, Desalination 284 (2012) 175–181.

[5] D. Wu, Y. Huang, S. Yu b, D. Lawless, X. Feng, Thin film composite nanofiltration membranes assembled layer-by-layer via interfacial polymerization from polyethylenimine and trimesoyl chloride, Journal of Membrane Science 472 (2014) 141–153.

[6] W. Suwaileh, D. Johnson, N. Hilal, Brackish water desalination for agriculture: Assessing the performance of inorganic fertilizer draw solutions, Desalination 456 (2019) 53–63.

[7] G. Zhang, W. Gu, Sh. Ji, Z. Liu, Y. Peng, Z. Wang, Preparation of polyelectrolyte multilayer membranes by dynamic layer-by-layer process for pervaporation separation of alcohol/water mixtures, Journal of Membrane Science 280 (2006) 727–733.

[8] P. Pardeshi, A. A. Mungray, Synthesis, characterization and application of novel high flux FO membrane by layer-by-layer self-assembled polyelectrolyte, Journal of Membrane Science 453 (2014) 202–211.

[9] Q. Saren, Ch. Q. Qiu, Ch. Y. Tang, Synthesis and characterization of novel forward osmosis membranes based on layer-by-layer assembly, Environ. Sci. Technol. 2011, 45, 5201–5208.

[10] Ch. Qiu, S. Qi, Ch. Y. Tang, Synthesis of high flux forward osmosis membranes by chemically crosslinked layer-by-layer polyelectrolytes, Journal of Membrane Science 381 (2011) 74– 80.

[11] J. Su, T. Chung, B. J. Helmer, J. S. de Wit, Enhanced double-skinned FO membranes with inner dense layer for wastewater treatment and macromolecule recycle using Sucrose as draw solute, Journal of Membrane Science 396 (2012) 92– 100.

[12] Ch. Liu, X. Lei, L. Wang, J. Jia, X. Liang, X. Zhao, H. Zhu, Investigation on the removal performances of heavy metal ions with the layer-by-layer assembled forward osmosis membranes, Chemical Engineering Journal 327 (2017) 60–70.

[13] W. Cheng, C. Liu, T. Tong, R. Epsztein, M. Sun, R. Verduzco, J. Ma, M. Elimelech, Selective removal of divalent cations by polyelectrolyte multilayer nanofiltration membrane: Role of polyelectrolyte charge, ion size, and ionic strength, Journal of Membrane Science. 559 (2018) 98–106.

[14] A. Akbari, H. Solymani, S. Majid M. Rostami, Preparation and characterization of a novel positively charged nanofiltration membrane based on polysulfone, Wiley Periodicals, Inc. J. Appl. Polym. Sci. 132 (2015) 41988.

[15] P. Kaner, D. J. Johnson, E. Seker, N. Hilal, S. A. Altinkaya, Layer-by-layer surface modification of polyethersulfone membranes using polyelectrolytes and AgCl/TiO2 xerogels, Journal of Membrane Science 493 (2015) 807–819.

[16] F. R. Omi, M. R. Choudhury, N. Anwar, A. R. Bakr, Md. S. Rahaman, Highly Conductive Ultrafiltration Membrane via Vacuum Filtration Assisted Layer-by-Layer Deposition of Functionalized Carbon Nanotubes, Ind. Eng. Chem. Res. 56 (2017) 8474−8484.

[17] Y. Li, Sh. Huang, Sh. Zhou, A.G. Fane, Y. Zhang, Sh. Zhao, Enhancing water permeability and fouling resistance of polyvinylidene fluoride membranes with carboxylated nanodiamonds, J. Membr. Sci. 556 (2018) 154–163.

[18] M. N. Chai, M. I. N. Isa, The Oleic Acid Composition Effect on the Carboxymethyl Cellulose Based Biopolymer Electrolyte, Journal of Crystallization Process and Technology, 3 (2013) 1-4.

[19] Y. Baek, J. Kang, P. Theato, J. Yoon, Measuring hydrophilicity of RO membranes by contact angles via sessile drop and captive bubble method: a comparative study, Desalination 303 (2012) 23–28.

[20] X. Jin, J. Shan, C. Wang, J. Wei, Ch. Y. Tang, Rejection of pharmaceuticals by forward osmosis membranes, J. Hazard. Mater. 227–228 (2012) 55–61.

[21] A. Tiraferri, N. Y. Yip, A. P. Straub, S. R. Castrillon, M. Elimelech, A method for the simultaneous determination of transport and structural parameters of forward osmosis membranes, J. Membr. Sci. 444 (2013) 523–538.

[22] P.V. O'neil, Advanced engineering mathematics, Seventh ed., Cengage learning, USA, 2011.

[23] M. Alvarez-Paino, A. M. Bonilla, G. Marcelo, J. Rodrıguez-Hernandez and M. Fernandez-Garcıa, Synthesis and lectin recognition studies of glycosylated polystyrene microspheres functionalized via thiol–para-fluorine ‘‘click’’ reaction, Polym. Chem. 3, (2012) 3282.

[24] L. Yu, Y. Zhang, B. Zhang, J. Liu, H. Zhang, Ch. Song, Preparation and characterization of HPEI-GO/PES ultrafiltration membrane with antifouling and antibacterial properties, Journal of Membrane Science 447 (2013) 452–462.

[25] Ch. Cheng, Sh. Li, W. Zhao, Q. Wei, Sh. Nie, Sh. Sun, Ch. Zhao, The hydrodynamic permeability and surface property of polyethersulfone ultrafiltration membranes with mussel-inspired polydopamine coatings, Journal of Membrane Science 417–418 (2012) 228–236.

[26] Z. Yang, X. Huang, J. Wang, Ch. Y. Tang, Novel polyethyleneimine/TMC-based nanofiltration membrane prepared on a polydopamine coated substrate, Chem. Sci. Eng. 12 (2) (2018) 273–282.

[27] Q. Nan, P. Li, B. Cao, Fabrication of positively charged nanofiltration membrane via the layer-by-layer assembly of graphene oxide and polyethylenimine for desalination, Applied Surface Science 387 (2016) 521–528.

[28] M. Ernst, A. Bismarck, J. Springer, M. Jekel, Zeta-potential and rejection rates of a polyethersulfone nanofiltration membrane in single salt solutions, Journal of Membrane Science 165 (2000) 251–259.

[29] R. H. Lajimi, E. Ferjani, M. S. Roudesli, A. Deratani, Effect of LbL surface modification on characteristics and performances of cellulose acetate nanofiltration membranes, Desalination 266 (2011) 78–86.

[30] J. T. Arena, B. McCloskey, B. D. Freeman, J. R. McCutcheon, Surface modification of thin film composite membrane support layers with polydopamine: Enabling use of reverse osmosis membranes in pressure retarded osmosis, Journal of Membrane Science 375 (2011) 55–62.

[31] Y. Zhou, S. Yu, C. Gao, X. Feng, Surface modification of thin film composite polyamide membranes by electrostatic self deposition of polycations for improved fouling resistance, Separation and Purification Technology 66 (2009) 287–294.

[32] M. Hu, B. Mi, Layer-by-layer assembly of graphene oxide membranes via electrostatic interaction, Journal of Membrane Science 469 (2014) 80–87.